Laser Wakefield Acceleration with Multi-Color Pulse Stacks:

Designer Electron Beams for Advanced Radiation Sources

Serge Kalmykov

Department of Physics & Astronomy, University of Nebraska – Lincoln, Lincoln, NE 68588-0299 USA

WG 1 – Electron beams from plasmas - 16 September 2015
EAAC 2015

Collaborators and funding

Xavier Davoine	CEA, DAM, DIF, Arpajon 91297, France
Rémi Lehe	LBNL
Agustin F. Lifschitz	LOA, ENSTA–CNRS–École Polytechnique UMR 7639, Palaiseau 91762, France
Isaac Ghebregziabher	Penn State
Bradley A. Shadwick	University of Nebraska – Lincoln

Inverse Thomson scattering simulations were completed utilizing the Holland Computing Center of the University of Nebraska.

S. K. and B. A. S. acknowledge stimulating discussions with Matthias Fuchs and the support from

U. S. Department of Energy Grant DE-SC0008382
National Science Foundation Grants PHY-1104683 and PHY-1535678

Outstanding task:

GeV laser-plasma acceleration with sub-Joule (10-TW-scale) laser pulses

Moderate average power:

- enables *high repetition rate* needed by applications that require high dosage (medicine, nuclear fluorescence studies *etc*.)

  1J @1 kHz = 1 kW — a hard, yet manageable laser engineering problem

- helps *reduce the size and cost of facilities*

- *lifts the barriers for first-principle modeling*

- enables *real-time control of the laser pulse phase* (using genetic algorithms) for optimization of the acceleration process

Plan of the talk:

1. Problems facing acceleration with Joule-energy pulses: Physical picture and outline of the solution.

2. Physics of dark current suppression – case study of linearly chirped, large-bandwidth drive pulse. Generating pulsed, quasi-monoenergetic MeV γ-rays via inverse Thomson scattering.

3. Pulse stacking – technically feasible path towards the optical control of the LPA. Robust GeV, low-background acceleration in mm-size plasmas. Generation of comb-like beams in plasma channels.

Acceleration in the blowout regime

Ultrasonic projectile: cavitation in a gas

Laser pulse in a plasma: cavitation of electron fluid

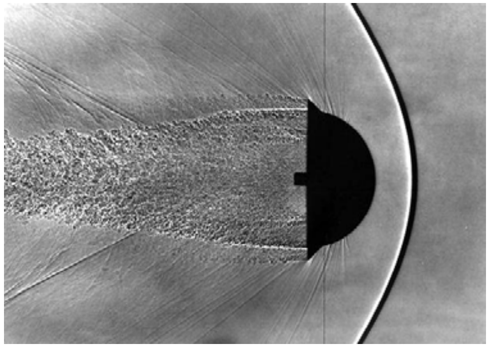

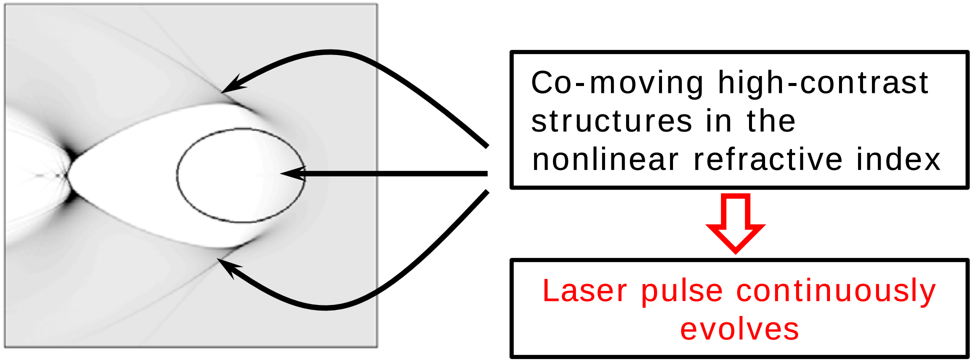

Accelerating bucket – electron density “bubble”– evolves in lock-step with the optical driver, responding to the variations in the ponderomotive force.

<u>Consequence 1</u>: Evolving bubble traps initially quiescent electrons and enforces their bunching/anti-bunching in phase space

<u>Consequence 2</u>: Manipulations of the laser pulse phase and amplitude may mitigate adverse optical processes, favorably changing bubble evolution, improving electron beam quality

***A clear path to*:**

- control injection process/electron phase space by purely optical means
- create “designer” beams tailored to the needs of applications

Single 10 TW-scale, <u>transform-limited</u> pulse is a bad choice for HQ, GeV acceleration☹

1. Guiding 10 TW-scale pulse needs a dense, highly dispersive plasma (~10^{19} cm^{-3})
2. Plasma response imparts large red-shift ($\Delta\lambda \sim \lambda_0$) at the pulse leading edge
3. Negative GVD compresses the pulse leading edge into a relativistic optical shock

Corollary 1: Pulse slows-down, dephasing length reduces, <u>energy gain drops to a 100-MeV level</u>

Corollary 2: Bubble continuously expands, trapping unwanted electrons, <u>polluting energy spectra with massive tails</u>

CALDER-Circ code:

VORPAL-PD code:

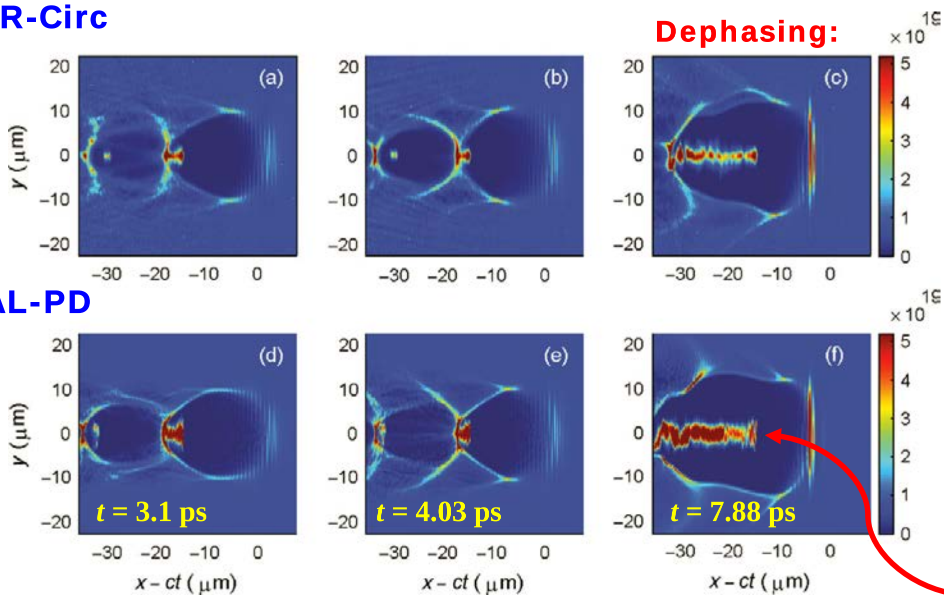

B. M. Cowan, S. Y. Kalmykov, A. Beck, X. Davoine *et al.*, *J. Plasma Phys.* **78**, 469 (2012)

Wavelength, λ_0	0.8 μm
Power / energy	70 TW / 2.1 J
TLD (FWHM in intensity)	30 fs
Plasma density, n_0	6.5×10^{18} cm^{-3}

E ≈ 420 MeV + huge tail

Pulse self-compression ⇒ bubble expansion ⇒ dark current

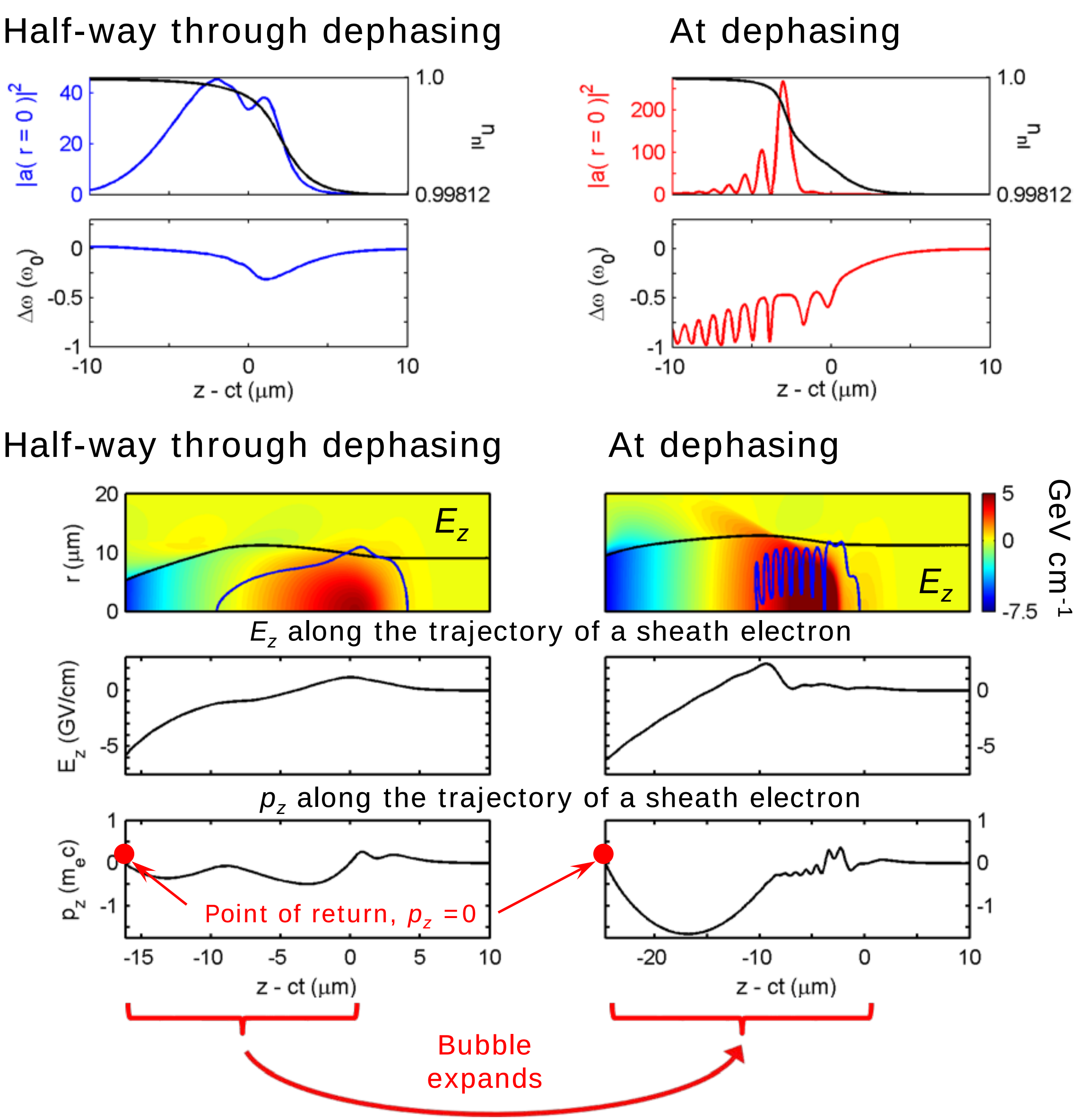

Formation of optical shock (OS) begins long before dephasing

Snow-plowing by the OS *piles up negative charge inside the shock*

Longitudinal electric field acting upon sheath electrons – injection candidates – increases multi-fold

Sheath electrons receiving stronger backward push at once become relativistic

⇒ their return to axis is delayed

⇒ bubble expands

<u>Corollaries</u>:

- Expansion of the bubble is a purely quasistatic phenomenon – plasma response to the drive pulse self-compression
- Mitigating self-compression eliminates the dark current.

Figures borrowed from S. Y. Kalmykov *et al*., NJP 14, 033025 (2012)
Simulation code: WAKE ⇒ PLASMA IS QUASISTATIC

Task: Prevent pulse self-compression
What is needed:

- large bandwidth of the drive pulse ($\Delta\lambda \sim \lambda_0$)
- temporal advancement of high frequencies (***negative chirp***).

These features:

- compensate for the nonlinear frequency red-shift
- slow down pulse self-compression
- take the energy tail down
- extend the dephasing length, increasing the energy gain far beyond predictions of accepted scaling (to the GeV level)

WHAT IS TO BE EXPECTED:

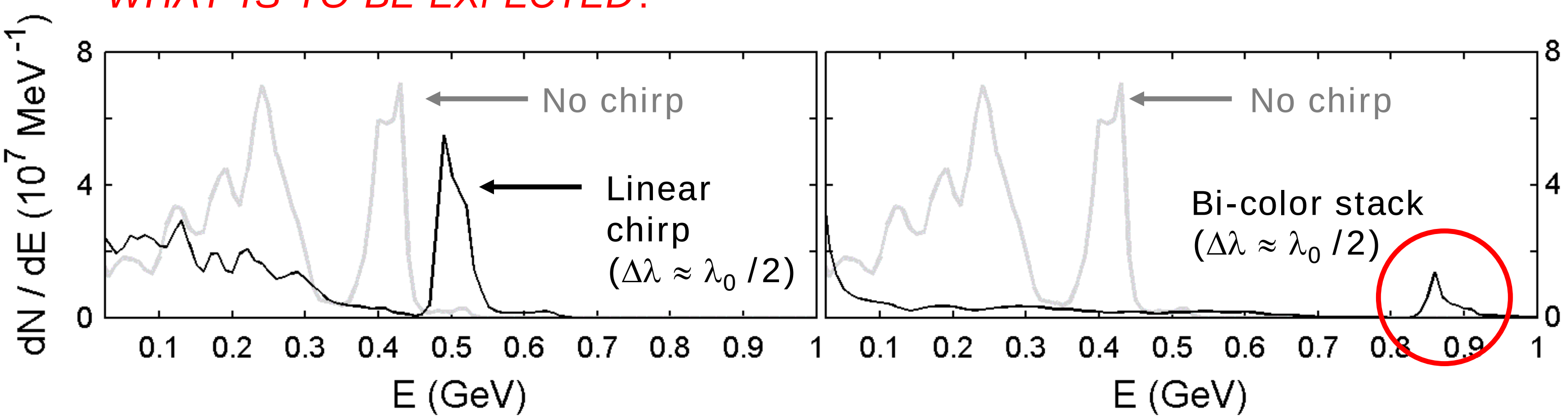

Technical option # 1: Joule-energy, broadband OPA

Review Article Vol. 1, No. 1 / July 2014 / Optica 45

Third-generation femtosecond technology

Hanieh Fattahi,[1,2] . . . ,[3 - 10] and Ferenc Krausz[1,2,*]

[1]Max-Planck Institut für Quantenoptik, Hans-Kopfermann-Str. 1, D-85748 Garching, Germany

[2]Department für Physik, Ludwig-Maximilians-Universität München, Am Coulombwall 1, D-85748 Garching, Germany

[3]Physics and Astronomy Department, King Saud University, Riyadh 11451, Saudi Arabia

[4]Current address: Electrical Engineering, Computer, Electrical and Mathematical Sciences and Engineering Division, Building 1, 4700 King Abdullah University of Science and Technology, Thuwal 23955-6900, Saudi Arabia

[5]TRUMPF Scientific Lasers GmbH + Co. KG, Feringastr. 10, 85774 München-Unterföhring, Germany

[6]Wigner Research Center for Physics, Konkoly-Thege Miklós út 29-33, H-1121 Budapest, Hungary

[7]Physics Department, POSTECH, San 31 Hyoja-Dong, Namku, Pohang, Kyungbuk 790-784, South Korea

[8]FFI (Norwegian Defence Research Establishment), Postboks 25, NO-2027 Kjeller, Norway

[9]Current address: Center for Nano-Optics (CeNO), Georgia State University, Atlanta, Georgia 30303, USA

[10]TRUMPF Laser GmbH + Co. KG, Aichhalder Str. 39, 78713 Schramberg, Germany

*Corresponding author: krausz@lmu.de

… Diode-pumped ytterbium-doped solid-state lasers … are able to deliver 1 ps scale pulses at kilowatt-scale average power levels, which, in thin-disk lasers, may come in combination with terawatt-scale peak powers. Broadband OPAs pumped by these sources hold promise for … the third-generation femtosecond technology (3FST) < that > offers the potential for femtosecond … multi-terawatt few-cycle pulses …

http://dx.doi.org/10.1364/OPTICA.1.000045

Vol. 1, No. 1 / July 2014 / Optica 46

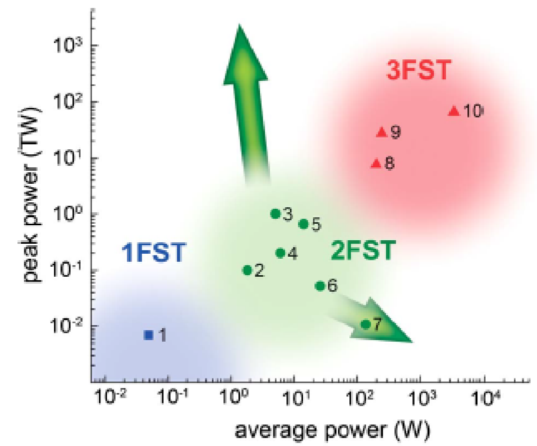

	τ_{pulse}	E_{pulse}	P_{peak}	$P_{average}$
system 8	5 fs	40 mJ	7.5 TW	200 W
system 9	1.7 fs	49 mJ	27 TW	245 W
system 10	5 fs	345 mJ	65 TW	3450 W

Fig. 1. Summary of recorded performances of 1FST and 2FST and the expected performance of 3FST, in terms of average and peak powers. … The blue square represents the best performance achieved by dye-laser technology (1, corresponding to Ref. [9]), the green dots show femtosecond CPA solid-state technology (2–7, corresponding to Refs. [60,71,66,18,67], and [25], respectively), and the red triangles represent the simulated results for OPCPA based on pump sources under development (8 and 9, pumped by a 1 ps, 5 kHz, 200 mJ Yb:YAG thin-disk laser) and envisioned (10, based on a future 1 ps, 10 kHz, 2 J Yb:YAG thin-disk laser system). …

NB: 5-10 kHz repetition rates!!

Expectations for the **system 10** (nominal parameters, pulse stretched to 20 fs, negatively chirped)

300 MeV in 0.5 mm @ $n_0 = 1.3 \times 10^{19}$ cm^{-3} ($\Delta E/E < 4\%$, weak tail),

Q = 35 – 50 pC, $\varepsilon_\perp^N < \pi$ mm mrad

S. Y. Kalmykov, X. Davoine, and B. A. Shadwick, *NIM A* **740**, 266 (2014)

Physics of dark-current suppression: Linear chirp

$\lambda_0 = 2\pi c / \omega_0$	Power/ energy	τ_L	r_0	$n_e\ (r = 0)$
0.8 μm	70 TW / 2.1 J	30 fs	13.6 μm	6.5×10^{18} cm^{-3}

Laser vector potential:

$$a(r, z=0, t) = a_0 \exp\left[-\left(\frac{r}{r_0}\right)^2 - 2\ln 2\left(\frac{t}{\tau_L}\right)^2 + i\varphi(t)\right]$$

$$\omega(t) = -\frac{\mathrm{d}\varphi}{\mathrm{d}t} = \omega_0 - 4\ln 2\left(\frac{\kappa}{\tau_L}\right)^2 t$$

Longitudinally uniform, leaky parabolic plasma channel:

$$n_e(r) = \begin{cases} n_0\left(1 + \dfrac{r^2}{r_{ch}^2}\right), & \text{for } r \le r_{ch} \\ 2n_0\left(2 - \dfrac{r}{r_{ch}}\right), & \text{for } r_{ch} < r \le 2r_{ch} \\ 0 & \text{for } r > 2r_{ch} \end{cases}$$

***Reference case*:**

Transform-limited pulse, $\kappa = 0$

***Negatively chirped pulse*:**

$\kappa = 2.4323$

($\tau_L = 5$ fs and $P = 420$ TW when fully compressed)

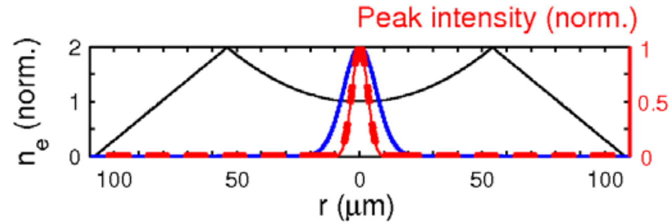

***Channel*:**

Matched to the self-guided spot size,

$r_{ch} = 38$ μm

or

$r_{ch} = \infty$ (flat plasma)

***Inverse Thomson scattering*:**

Interaction pulse: linearly polarized, $r_0 = 20$ μm; $a_0 = 0.1$; $\lambda = 0.8$ μm; FWHM 250 fs.

Detector: on axis, scattering angle = π.

Simulation: fully relativistic PIC codes & particle tracker for radiation calculation

- Exploring optical beam evolution in the plasma and beam loading effects: **WAKE** (extended-paraxial, ponderomotive guiding center, quasi-static)

  [P. Mora and T. M. Antonsen, Jr., Phys. Plasmas 4, 217 (1997)]

- Accurate simulation of self-injection and acceleration: **CALDER-Circ** (quasi-cylindrical, fully explicit; poloidal mode decomposition of fields and currents)

  [A. F. Lifschitz, X. Davoine et al., J. Comp. Phys. 228, 1803 (2009)]

  Also: numerical Cherenkov-free EM solver; 2nd or 3rd order macro-particles

  [R. Lehe, A. F. Lifschitz et al., Phys. Rev. ST Accel. Beams 16, 021301 (2013)]

- Inverse Thomson scattering code

  [I. A. Ghebregziabher, B. A. Shadwick et al., Phys. Rev. ST Accel. Beams 16, 030705 (2013)]

  fully relativistic particle tracker; laser beam is paraxial; radiation calculation using classical formula

$$\frac{d^2 I}{d\omega d\Omega} = 2|\mathbf{A}(\omega)|^2, \qquad \mathbf{A}(\omega) = \left(\frac{e^2}{8\pi^2 c}\right)^{1/2} \int_{-\infty}^{\infty} e^{i\omega t}\left[\frac{\mathbf{n}\times[(\mathbf{n}-\boldsymbol{\beta})\times\dot{\boldsymbol{\beta}}]}{(1-\boldsymbol{\beta}\cdot\mathbf{n})^3}\right]dt, \qquad \frac{d^2 I_e}{d\omega d\Omega} = \frac{1}{N_s}\sum_{i=1}^{N_s}\frac{d^2 I_i}{d\omega d\Omega}.$$

Effect of negative chirp: Suppressing bubble expansion

TLP: uniform plasma | NCP: uniform plasma | NCP: plasma channel

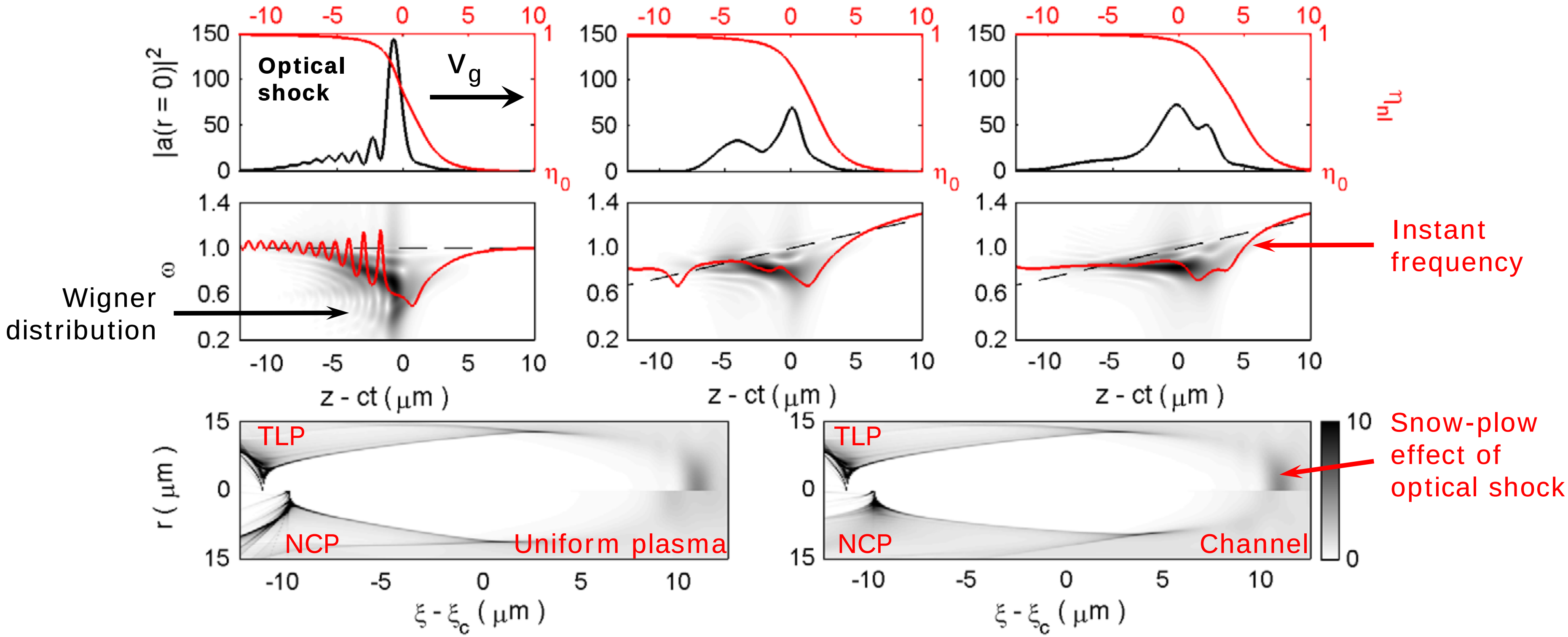

z = 1.72 mm (70% of dephasing length)

Electron spectra (CALDER-Circ)

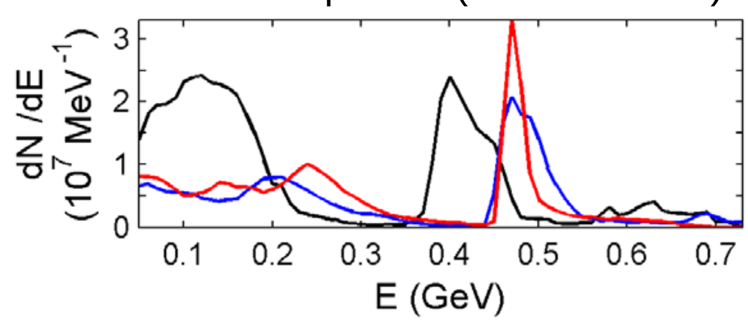

TLP – uniform plasma

NCP – uniform plasma

NCP – plasma channel

(WAKE simulations except the energy spectra)

NCP: Acceleration through dephasing (uniform plasma)

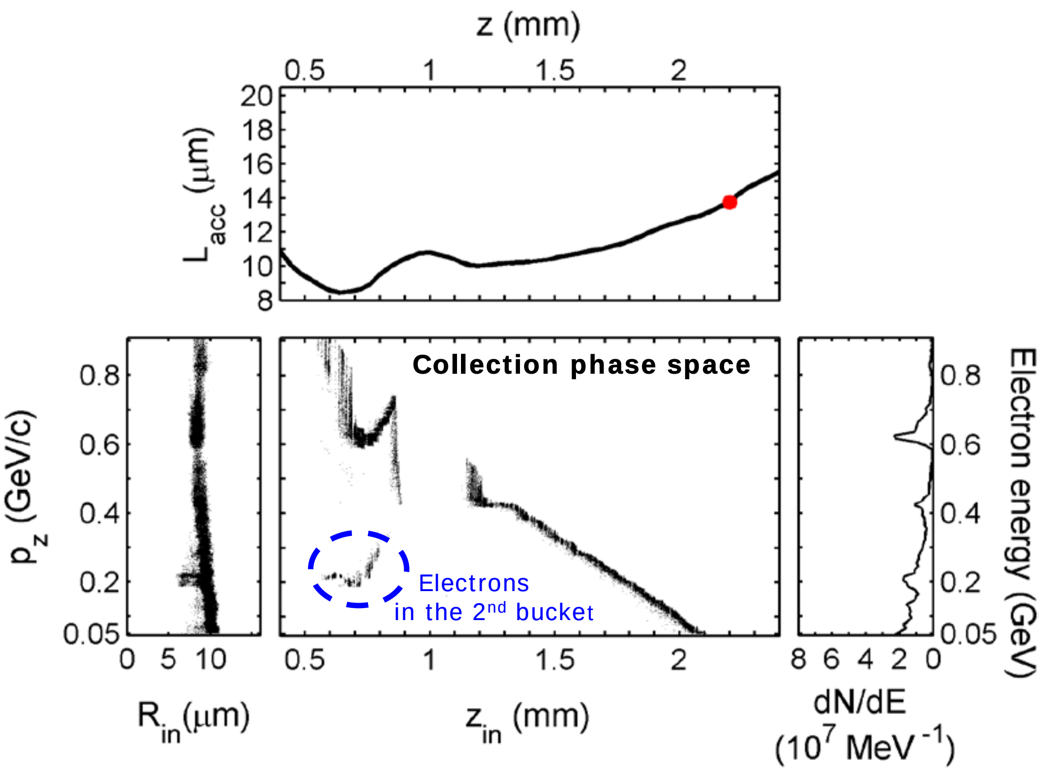

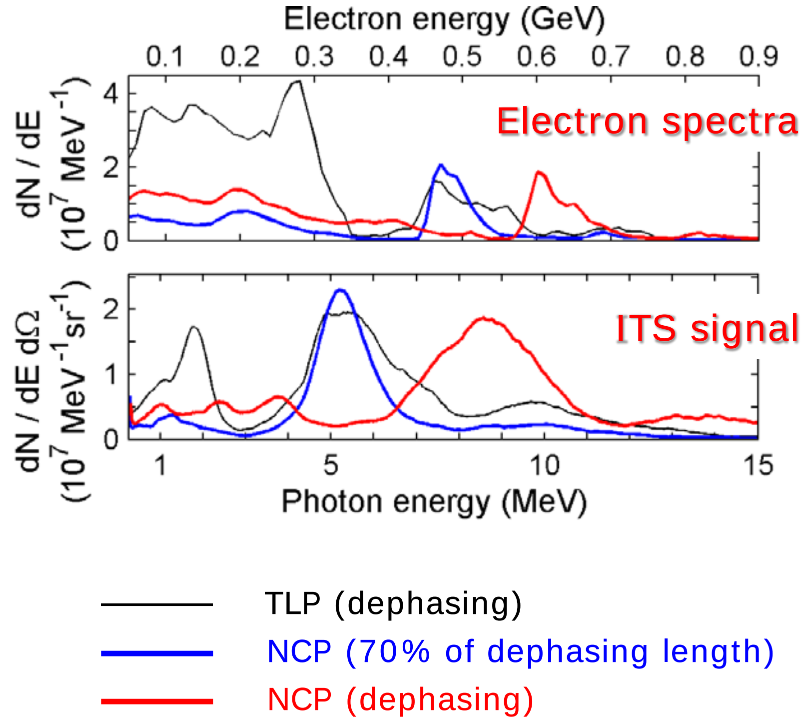

Energy spread of the ITS signal is dominated by mrad divergence of e-beam

NCP vs Reference: Electron energy tail is down (0.4× charge, 0.3× flux)

Mean energy of the signal is up (+ 20%);

the energy spread is down (- 30%);

normalized transverse emittance preserved (0.57 mm mrad).

Yet, there is a remnant of a tail (not incompatible with the ITS application).

Propagating the NCP <u>in a channel</u> splits the tail into QME bunches.

(CALDER-Circ simulation)

Accordion effect in a channel: periodic injection and multi-bunching in phase space

Channel upsets the balance between the radiation pressure and charge separation force in the pulse tail area

Tail flaps ⇒ Bubble size oscillates ⇒ 3 bunches in the 1st bucket (absorbing 16.5% of laser energy)

(WAKE simulation)

(CALDER-Circ simulation)

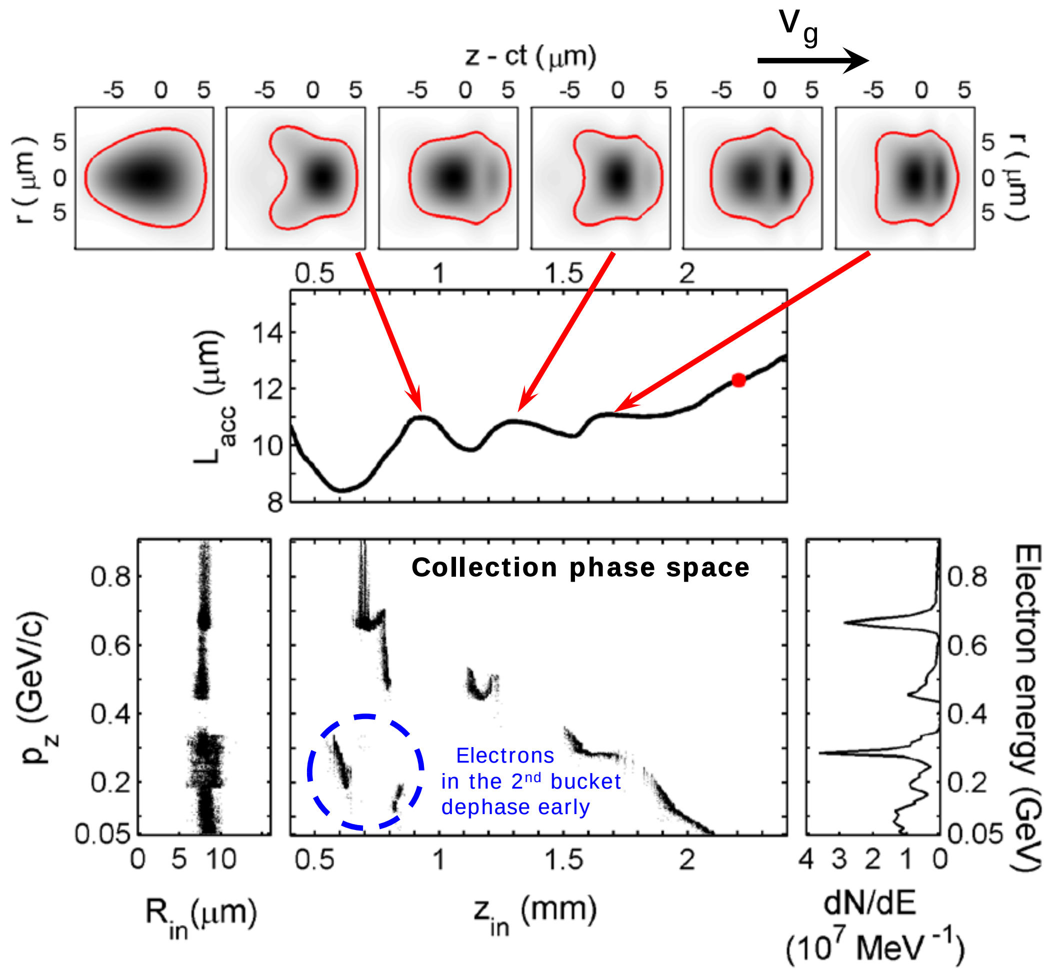

Comb-like electron beams from the channel: Generating polychromatic, pulsed inverse-Thomson γ-rays

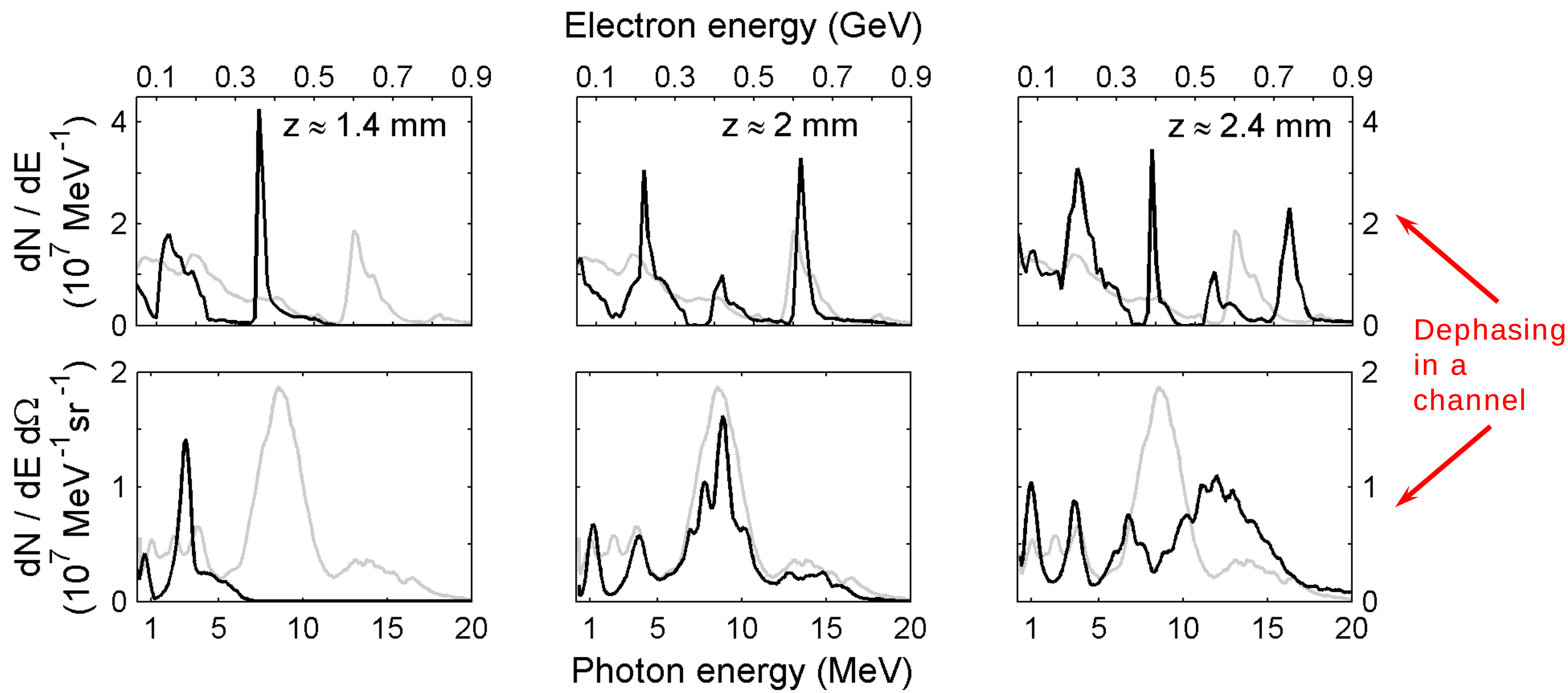

Gray: NCP in the uniform plasma (z = 2.16 mm; dephasing)

Black: NCP in the channel matched to the self-guided spot size

By dephasing, *four injections in the first bucket* yield four distinct, fs-length electron bunches with

$\varepsilon_{\perp}^{N}$ ~ 1 mm mrad (conserved up to a third digit)

0.75 – 1.5 mrad divergence

relative energy spread 5–15%

Multi-color γ-rays from comb-like beams

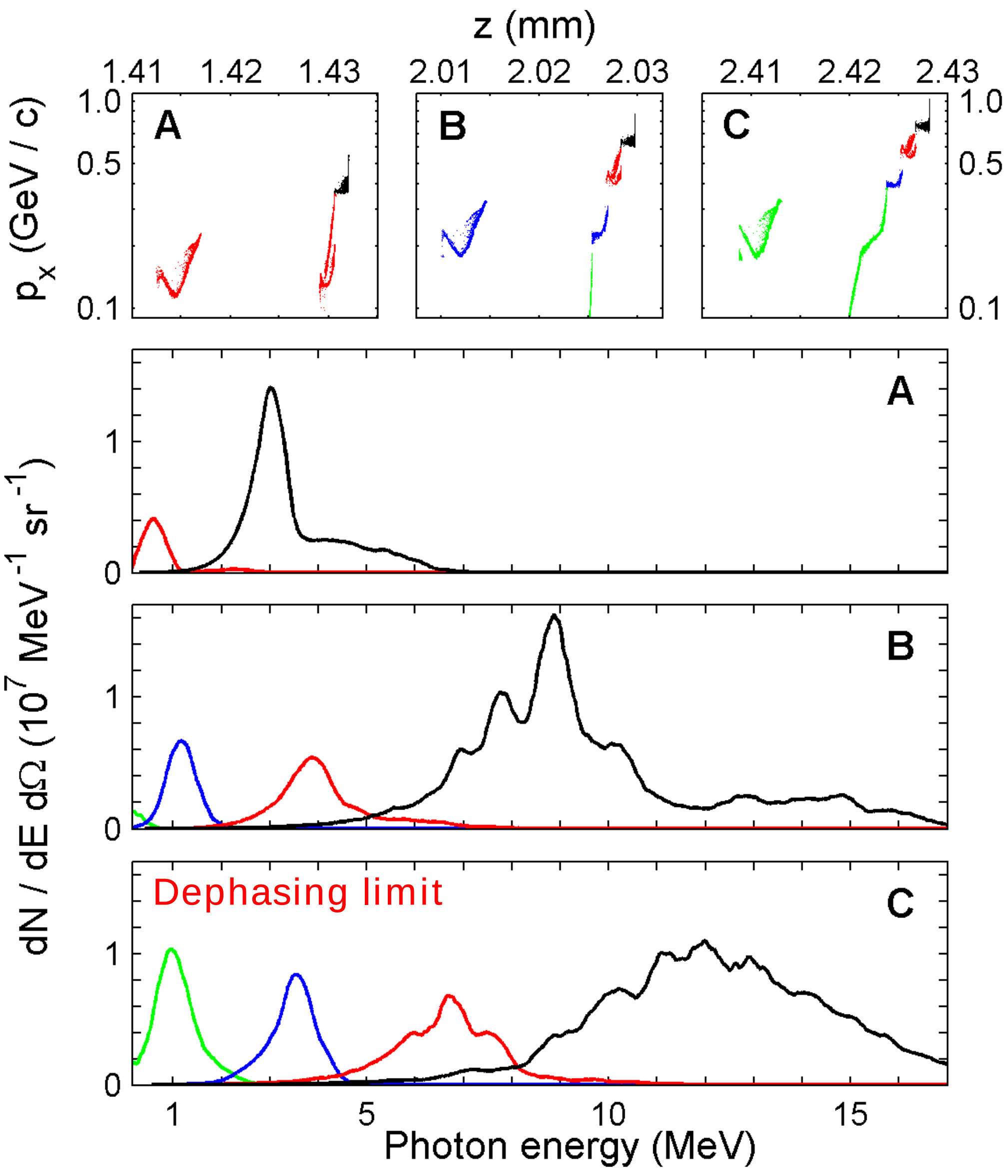

In the course of acceleration, transverse emittance of individual bunches (~ 1 mm mrad) varies in the third digit.

Extracting background-free comb-like beams from plasma at ≈ 1.4, 2, 2.4 mm yields drivers for bi-, tri-, four-color pulsed ITS γ-ray source (equally background free).

Mrad divergence of individual bunches dictates 20 – 30% energy spread of partial ITS signals.

Separating fs-length components of the comb using magnets and using delay lines may help synchronize them (and γ-ray flashes) at various pre-selected delays.

Quasi-monoenergetic acceleration in the channel

Physical solution: Clip the pulse tail – reduce the amount of radiation confined in the bubble

Practical approach: Compress the pulse (as permitted by the large bandwidth)

Results are shown for 20 fs, 70 TW NCP in a wide channel (matched to the incident pulse)

Accordion effect eliminated!

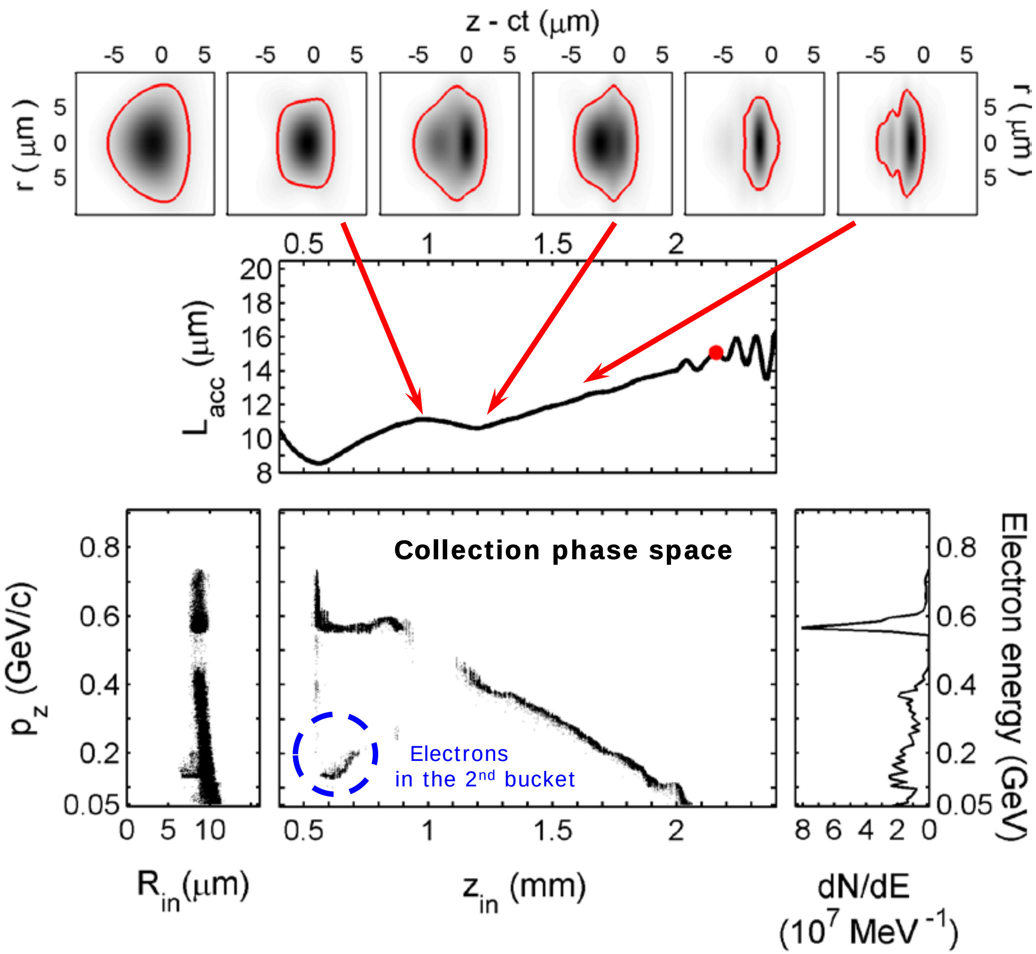

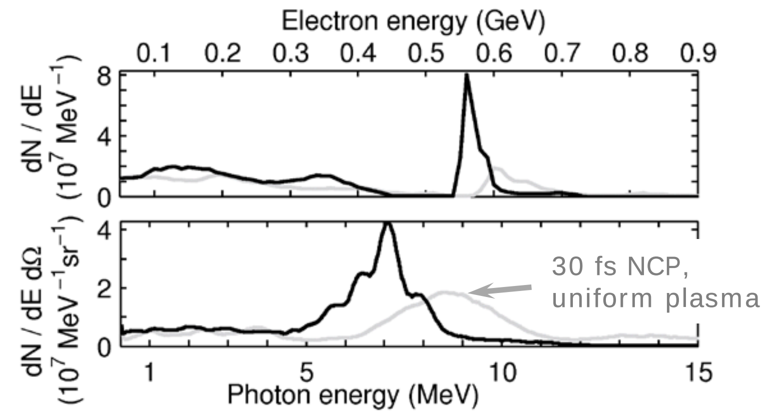

Compressing the pulse:

- restores the quasi-monoenergetic signal (absorbing 16% of laser energy)
- increases electron and γ-ray flux
- keeps the background low (same as in the uniform plasma).

Technical option #2:

Stacking sub-Joule, transform-limited pulses of different colors

Linearly chirped, 100-TW scale optical pulses with the bandwidth $\Delta\lambda \sim \lambda_0$ are not immediately available.

Fortunately, the effect is not too sensitive to the exact shape of the chirp.

Technological options available in the near-term afford building a large-bandwidth NCP (with a step-wise chirp) by stacking collinearly propagating pulses from conventional CPA.

Pulses must be frequency-shifted, with the amount of frequency blue-shift (comparable with ω_0) dictated by the LPA optimization routine and availability of technological options:

- Frequency shift in Raman cells with subsequent conventional CPA
  [F. B. Grigsby, P. Dong, and M. C. Downer, JOSA B 25, 346 (2008)]
- Energy-efficient methods of 2^{nd} harmonic pulse generation.

This photon engineering opens new venues towards (quasi-monoenergetic) GeV acceleration with Joule-energy pulses, with standard target design (a few mm-long gas jets, cells, or channels)

Purpose of stacking:
Protecting the pulse from nonlinear erosion

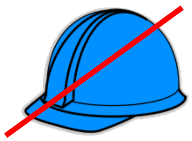

Optical shock forms: the pulse smashes its head long before electron dephasing!

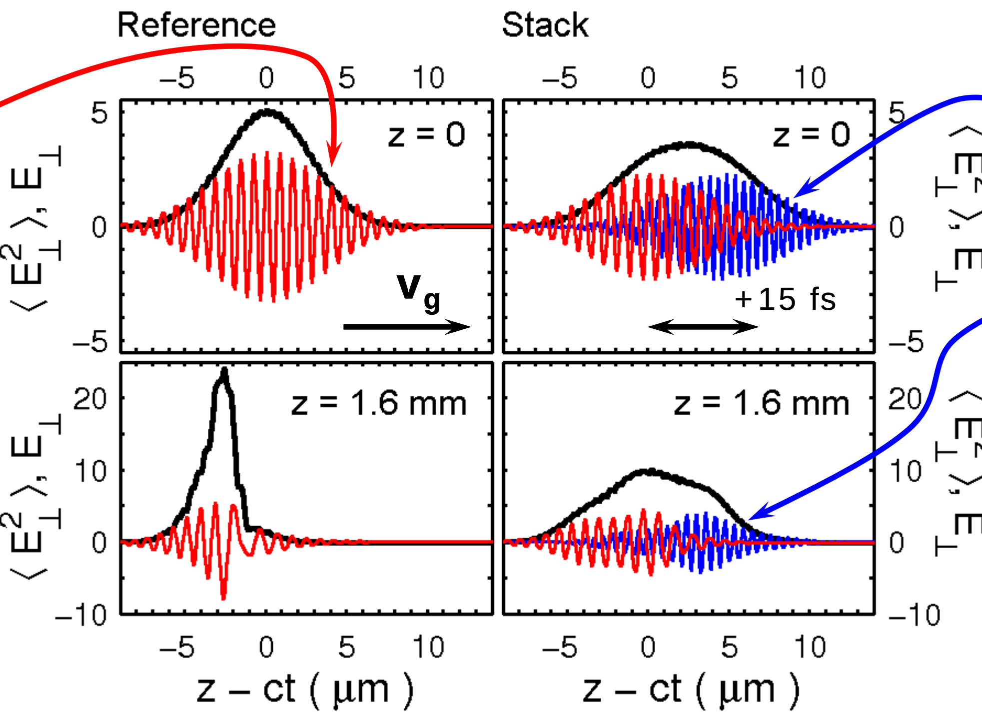

Blue-shifted “hard-hat” protects the pulse

Pulse head is intact (no optical shock)!

Pulse 1: 20 fs, 2.1 J, λ_1 = 0.8 μm

Pulse 2: 20 fs, 0.7 J, λ_2 ≈ 0.5 μm

} orthogonally polarized (incoherent mixing)

No need in the extreme frequency up-shift: Reducing λ_2 by 20% is sufficient!

(CALDER-Circ simulation)

Benefits of stacking – I: reducing depletion, red-shift, increasing dephasing length

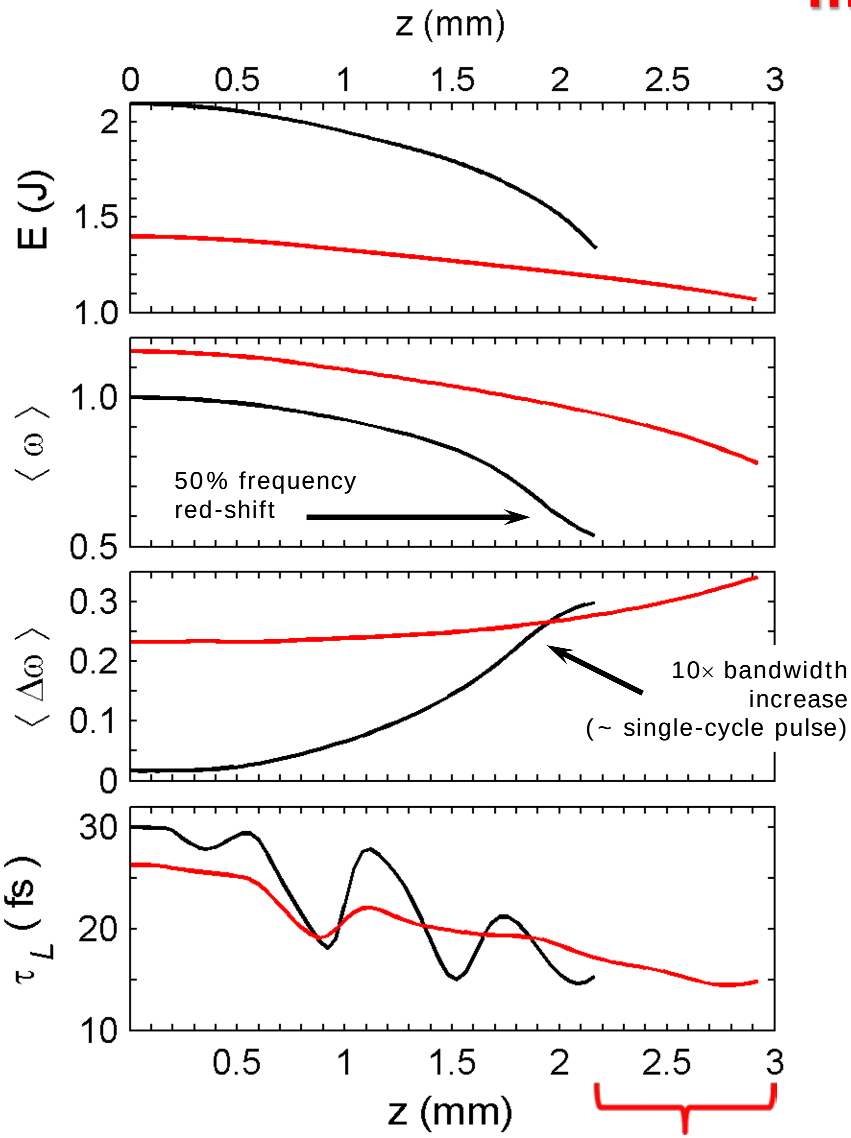

60% increase in dephasing length

(WAKE simulation)

- Extreme negative chirp reduces energy depletion

- reduces the average red-shift

$$\langle \omega(z) \rangle = \int_0^\infty r\,\mathrm{d}r \int_0^\infty \omega |a(r,z,\omega)|^2 \mathrm{d}\omega \left(\omega_0 \int_0^\infty r\,\mathrm{d}r \int_0^\infty |a(r,z,\omega)|^2 \mathrm{d}\omega \right)^{-1}$$

$$a(r,z,\omega) = \mathrm{F}[a(r,z,\xi)], \quad \xi = ct - z$$

- preserves the RMS bandwidth

$$\langle \Delta\omega(z) \rangle^2 = \int_0^\infty r\,\mathrm{d}r \int_0^\infty (\omega - \langle \omega \rangle)^2 |a(r,z,\omega)|^2 \mathrm{d}\omega \left(\omega_0^2 \int_0^\infty r\,\mathrm{d}r \int_0^\infty |a(r,z,\omega)|^2 \mathrm{d}\omega \right)^{-1}$$

- reduces self-compression

$$\langle \tau(z) \rangle = \int_{-\infty}^{\infty} \xi |a(0,z,\xi)|^2 \mathrm{d}\xi \left(c \int_{-\infty}^{\infty} |a(0,z,\xi)|^2 \mathrm{d}\xi \right)^{-1}$$

$$\langle \Delta\tau(z) \rangle^2 = 8 \ln 2 \int_{-\infty}^{\infty} (\xi - c\langle \tau \rangle)^2 |a(0,z,\xi)|^2 \mathrm{d}\xi \left(c^2 \int_{-\infty}^{\infty} |a(0,z,\xi)|^2 \mathrm{d}\xi \right)^{-1}$$

Reference case (30 fs, 70 TW TLP)

Bi-color stack with λ_1 = 0.8 μm, λ_2 = 0.53 μm

Benefits of stacking – II: Dark current eliminated, electron energy boosted

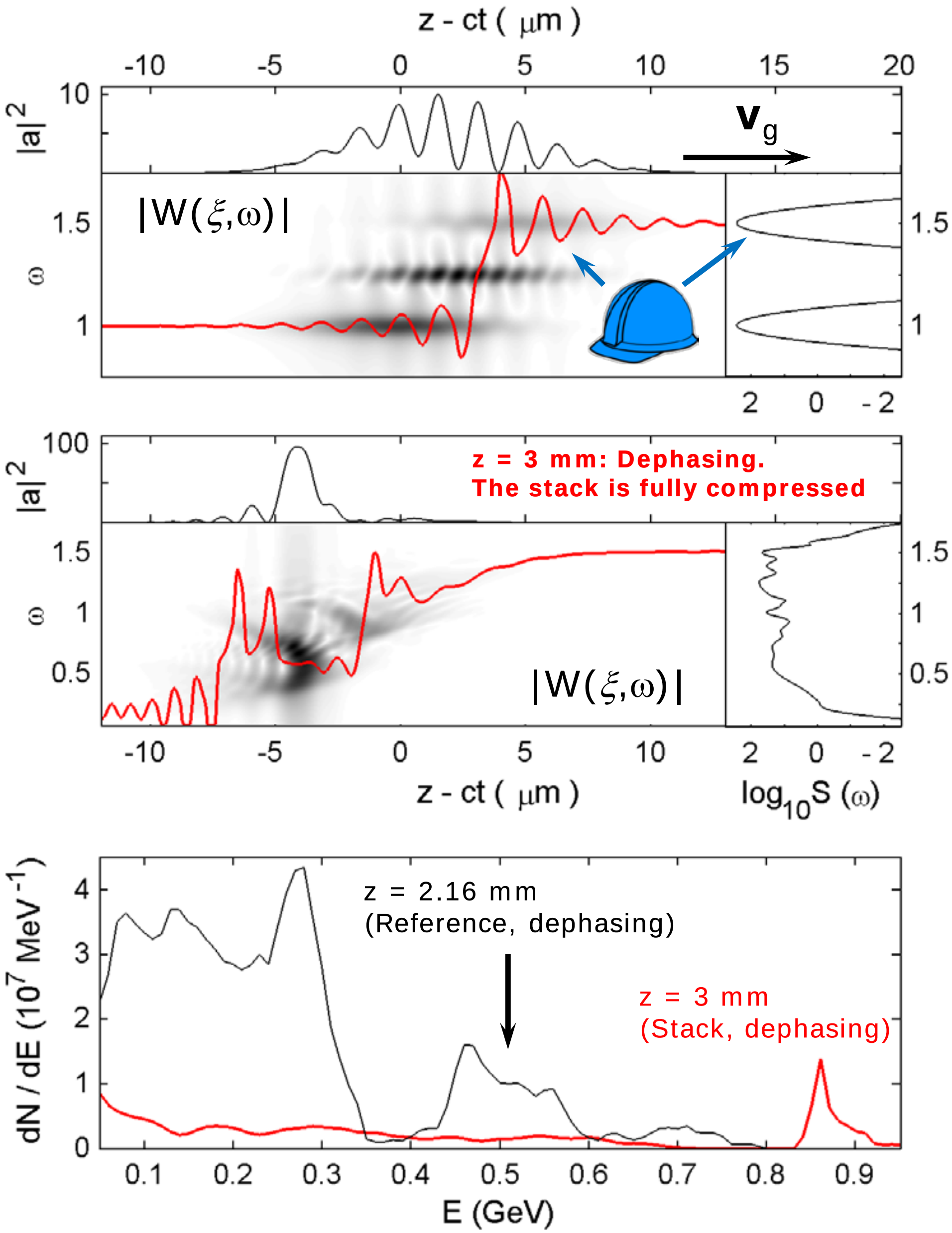

1. Stack remains uncompressed through electron dephasing
2. Dephasing length increases by 60%
3. **Flux in the energy tail drops, on average, by a factor 10**
4. **Electron energy increases by 75%!**
5. Normalized transverse emittance drops by 20% (to 0.4 mm mrad)

   RMS energy spread drops by 45% (to 30 MeV)

   Charge drops by a factor 3.75 (to 75 pC)
6. Current (≈ 85 kA) and peak flux are preserved

The stack: 0.7/0.7 J, delay +15 fs, $\lambda_2 = 2/3\ \lambda_1 = 0.53\ \mu m$

Stack vs. Reference: Dynamics of self-injection

Self-injection process
(CALDER-Circ simulations):

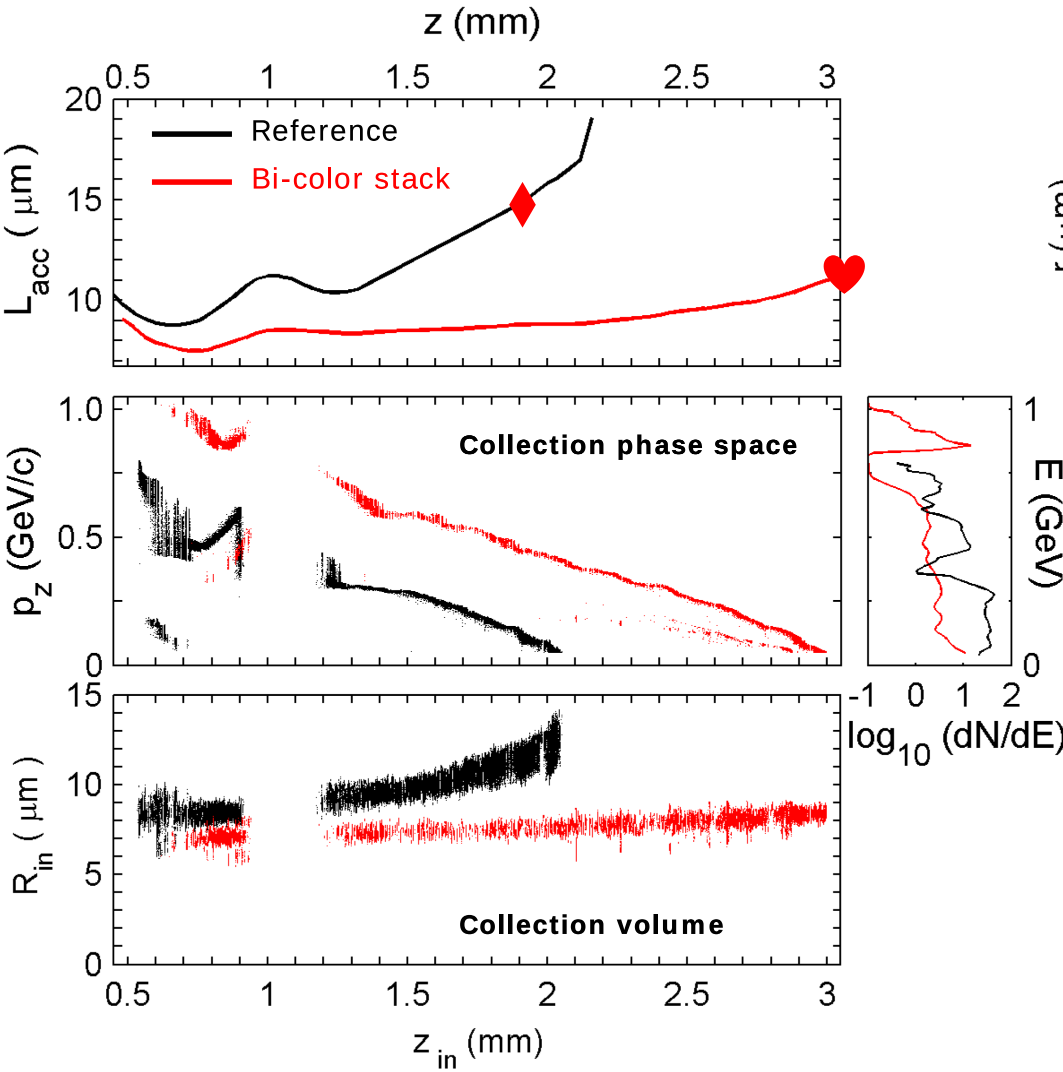

Quasi-static bubble at the point
of full pulse compression
(WAKE simulations):

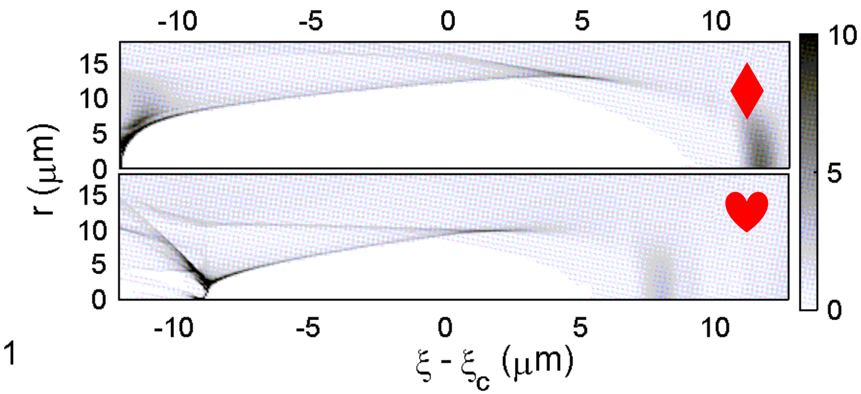

Much slower self-compression of
the stacked driver leads to:

- extremely slow expansion of the bucket
- almost negligible accumulation of charge in the tail

Robust GeV-scale stacked-pulse LPA - I:

Energy equipartition, fixed frequency difference, variable delay

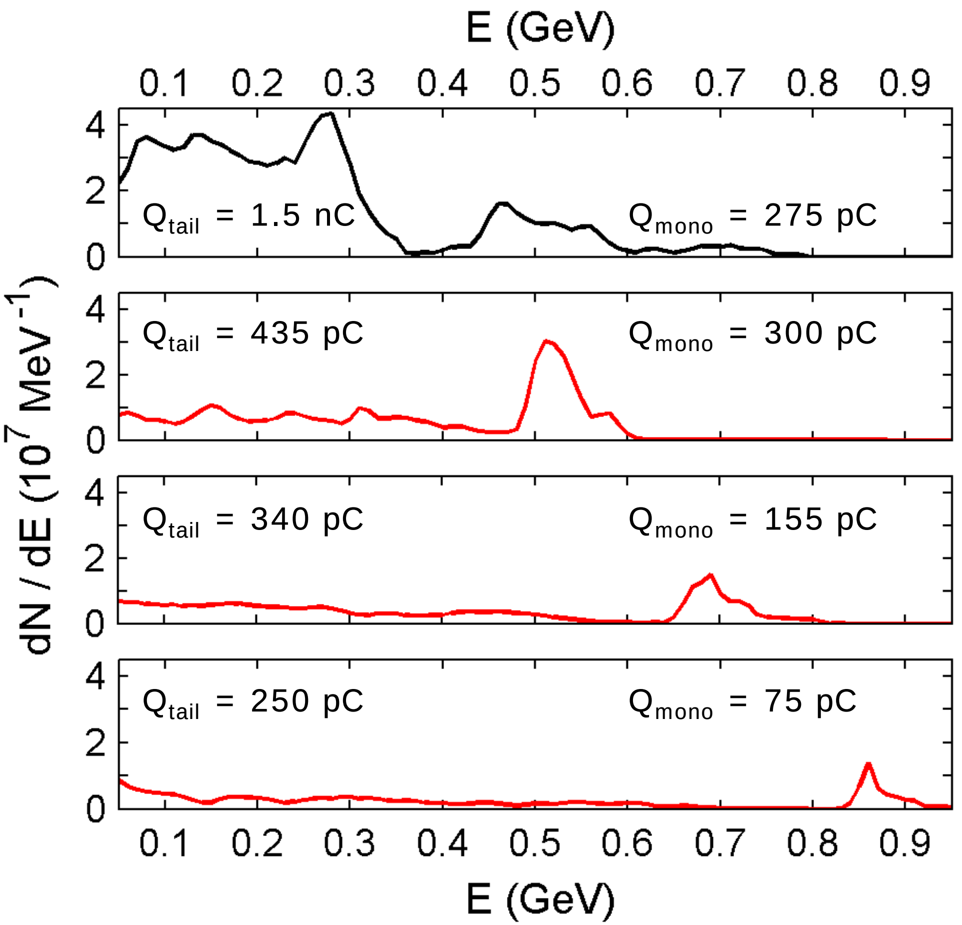

Stacks with $\lambda_2 = 2/3\lambda_1 = 0.53\ \mu m$,
$E_1 = E_2 = 0.7$ J

Delay:

0 fs

+10 fs

+15 fs (optimal)

Trade-off between the accelerated charge and final energy

<u>Reduced beam loading accounts for merely 25% of the energy boost!!</u>

Acceleration through dephasing with a variable-delay stack produces electron beams with:

- Energy efficiency: 5 – 15% of the laser energy is transferred to the QM bunch
- Brightness: 1.5 – 2.7 × 10^{14} part. MeV^{-1} mm^{-2} mrad^{-2} (1.5 × 10^{14} for Reference)

Robust GeV-scale stacked-pulse LPA - II:

Energy equipartition, variable frequency difference, fixed delay

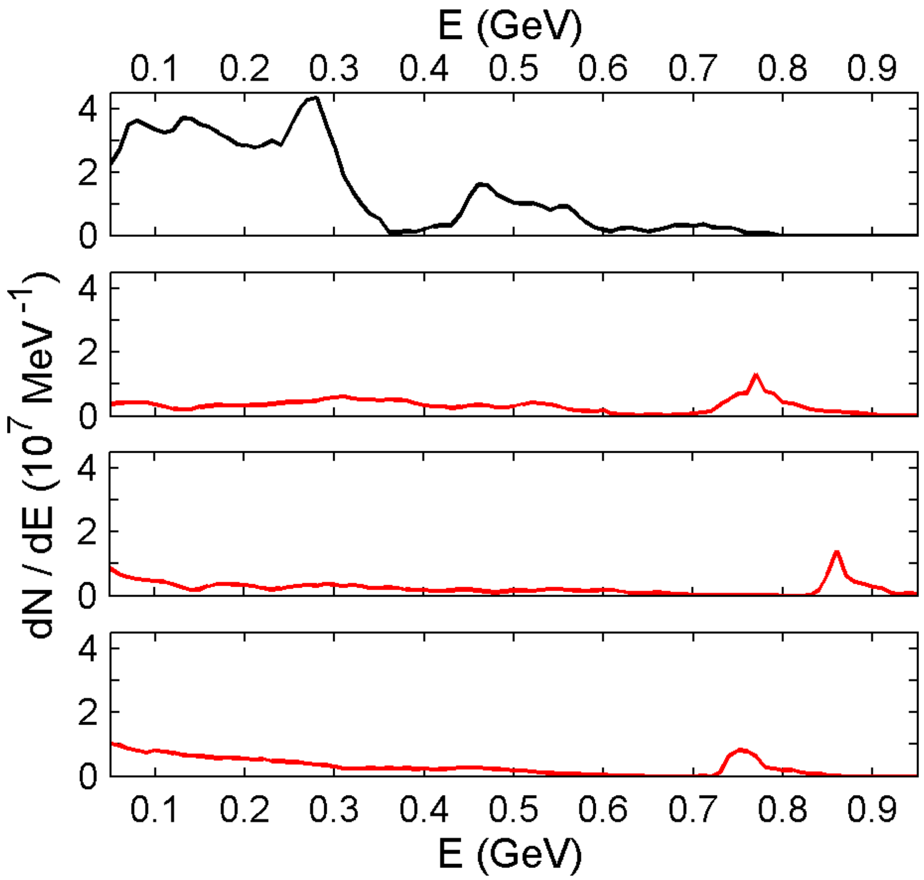

Stacks with a +15 fs delay,
$\lambda_1 = 0.8\mu m$, $\mathbf{E_1 = E_2 = 0.7\ J}$

$\lambda_2 = 0.8\ \lambda_1 = 0.64\ \mu m$

$\lambda_2 = 2/3\ \lambda_1 = 0.53\ \mu m$ (optimal)

$\lambda_2 = \lambda_1/2 = 0.4\ \mu m$ — the 2nd harmonic!

The result of acceleration is not too sensitive to the amount of blue-shift, as soon as it is large enough (20-100%) $\Rightarrow$ flexibility in technical solutions that permit those shifts (Raman cells, second-harmonic generation)

Robust GeV-scale stacked-pulse LPA - III:

Unequal energy partition, fixed frequency difference, variable delay

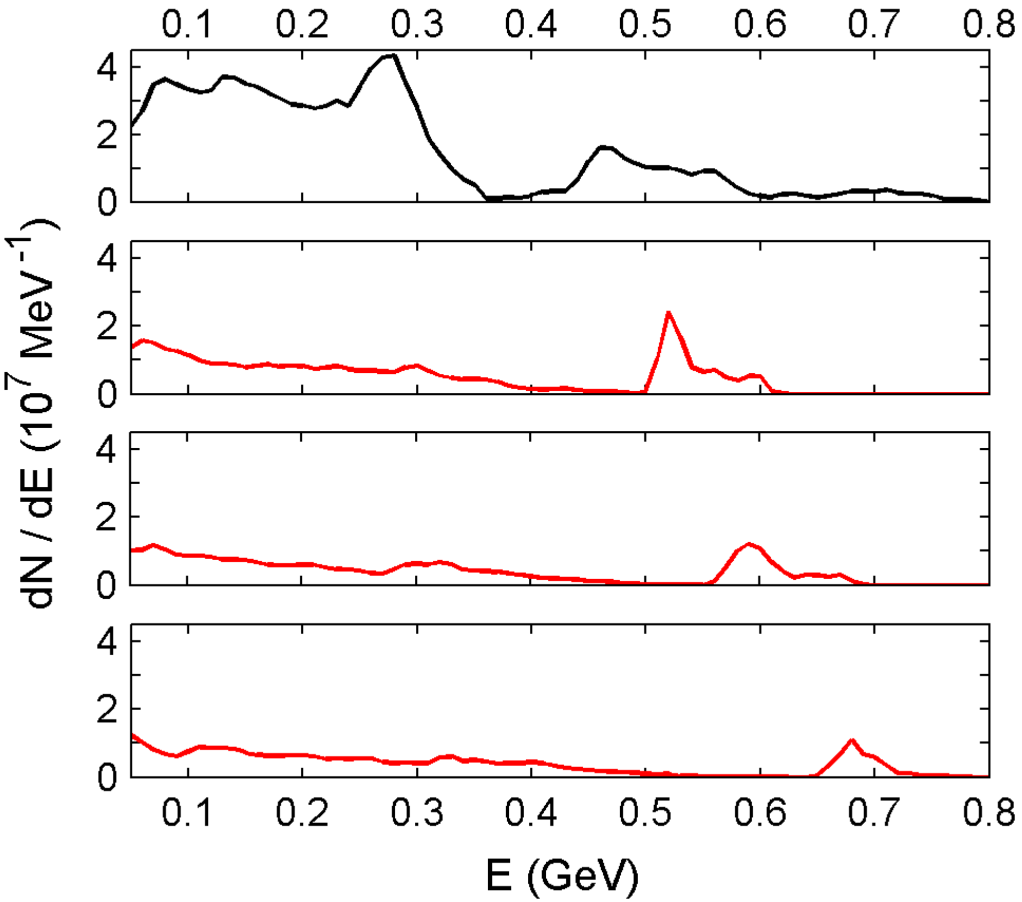

Stacks with $\lambda_2 = 2/3\lambda_1 = 0.53\ \mu m$,
$E_1 = 0.7$ J, **$E_2 = 0.31$ J**

$\Delta T = 10$ fs

15 fs

20 fs

Reducing the energy of the blue-shifted "hard hat" by more than 50% preserves low-background acceleration (the energy gain drops by ~ 25%).

Robust GeV-scale stacked-pulse LPA - IV:

Dense plasma ($\geq 10^{19}$ cm^{-3}), 100-mJ scale pulses

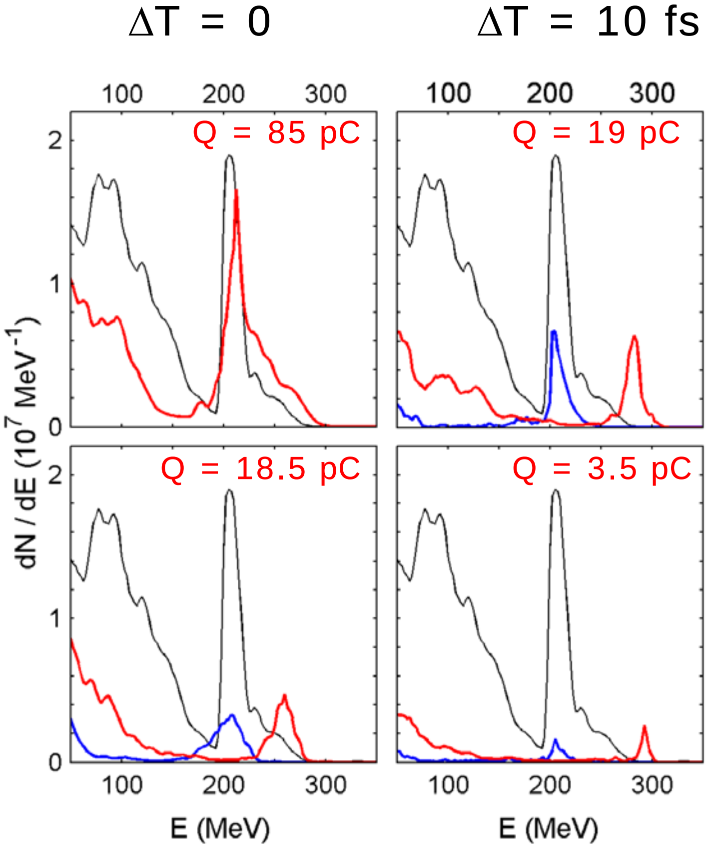

$\omega_1 = 1.25\omega_0$

$\omega_1 = 1.5\omega_0$

Plasma density: 1.3×10^{19} cm^{-3}

Stack of 20 fs pulses with

$\lambda_0 = 0.8\ \mu$m

$r_0 = 5.75\ \mu$m

$E_1 = E_2 = 0.15$ J

In all stacked cases, at dephasing,

90% of the tail charge is below 150 MeV,

peak signal ranging from 210 to 295 MeV,

$\varepsilon_\perp^N \sim$ 0.35 to 1.05 mm mrad

Reference (dephasing, Q = 77 pC)

Stacks (matching peak energy in the Reference case)

Stacks (dephasing, $z_d \approx$ 0.6 to 0.7 mm)

Optimal stack in a channel — I: Periodic injection and multi-bunching in phase space

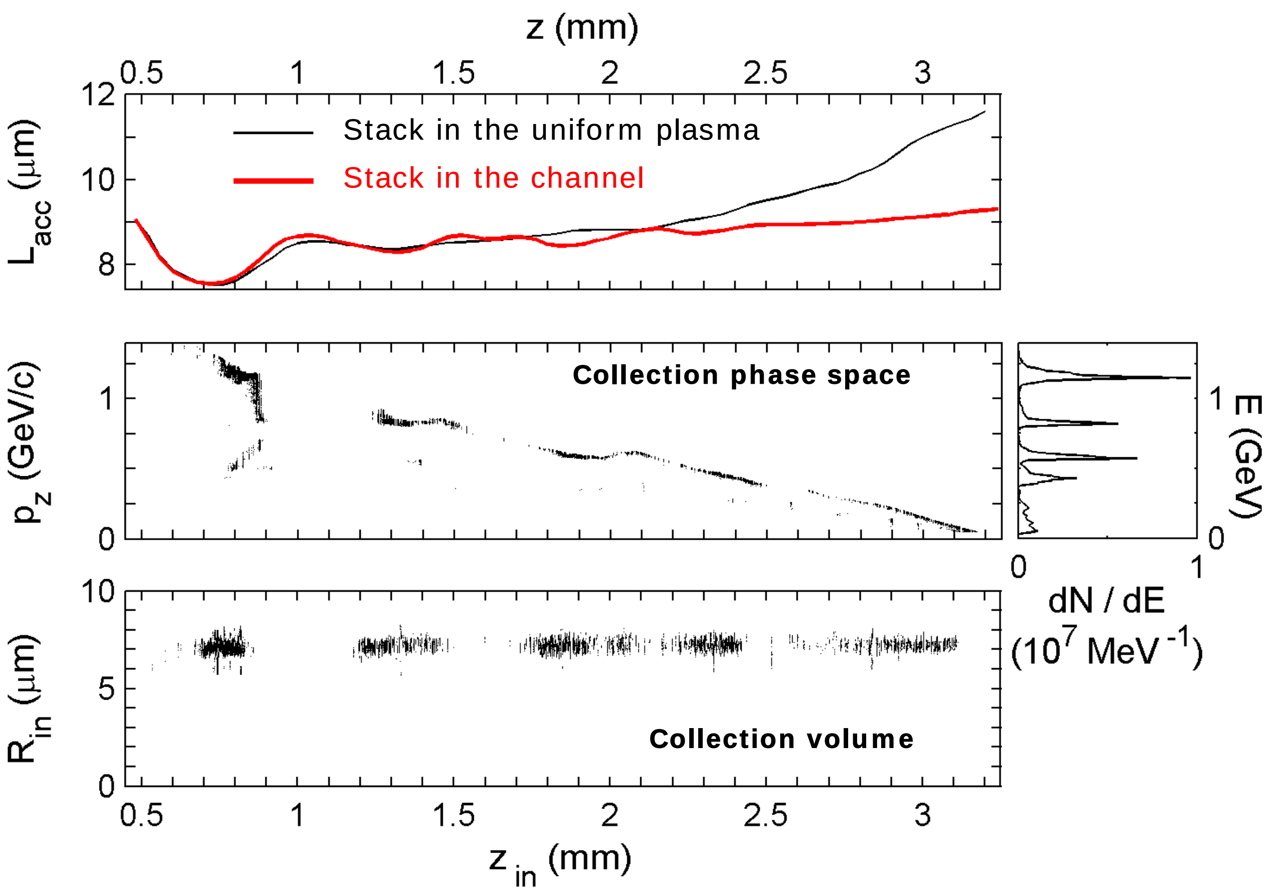

Stack with
+15 fs delay,
λ_2 = 2/3 λ_1 = 0.53 μm,
E_1 = E_2 = 0.7 J,
in a channel matched to the incident pulse waist

The channel:

- suppresses diffraction of the pulse head, further delaying self-compression
- destabilizes the pulse tail confined within the bubble, causing periodic injection
- a comb of synchronized, kA-current bunches is produced (no tail at all!!)
- **peak energy ~ 1.2 GeV (vs ~ 420 MeV from accepted scaling)**

Optimal stack in a channel — II: Progress through dephasing

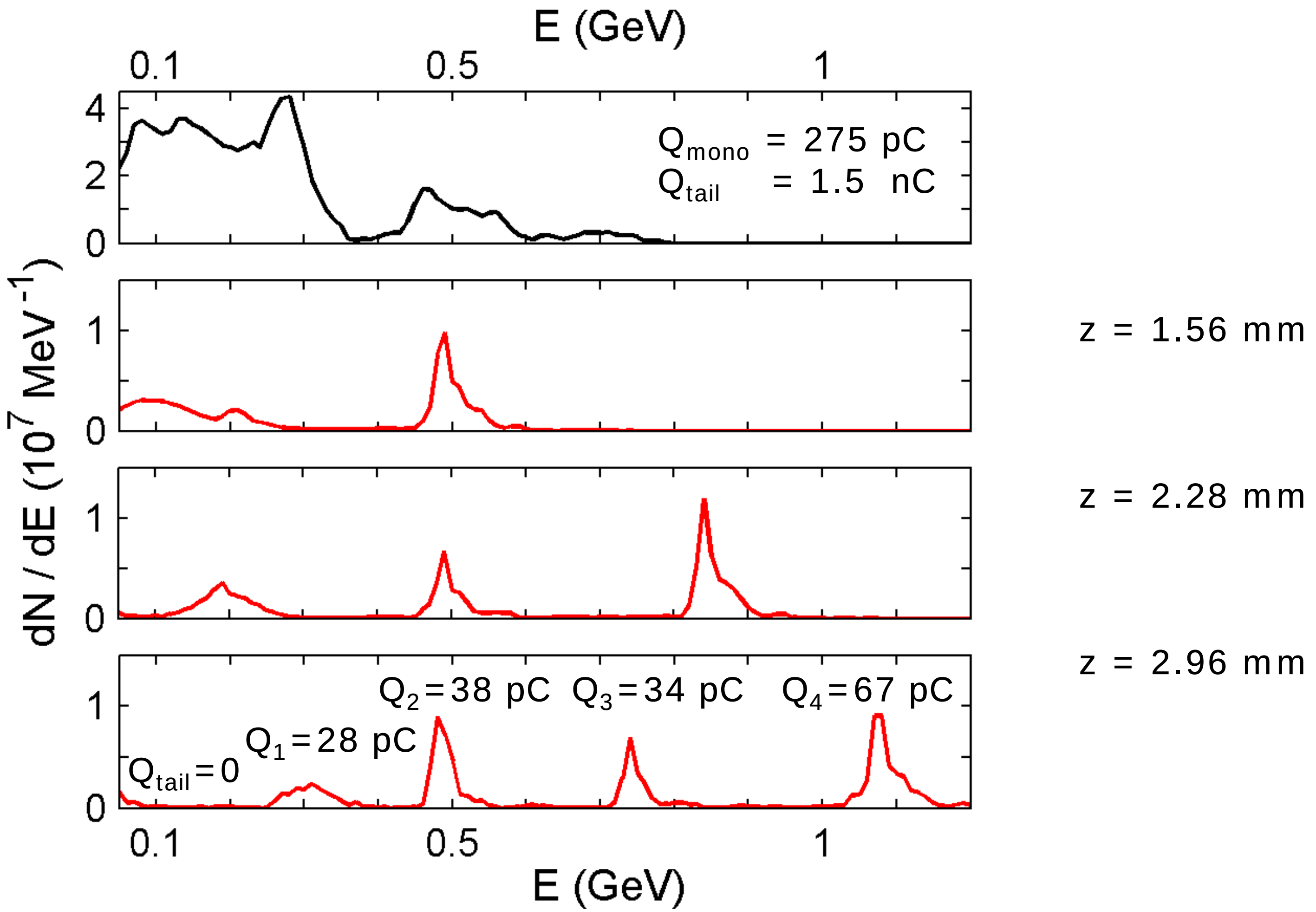

10% of laser energy is transferred to the 4-component comb-like beam

Varying the channel length controls the number of components in the comb, their energy and energy difference without compromising their quality:

sub-fs length, 35-100 kA current,
1-2 mrad RMS divergence, 0.3-0.6 mm mrad normalized transverse emittance.

Stack in a channel — energy equipartition (0.7 / 0.7 J)

Electron energy spectra are shown at dephasing

Frequency of “hard hat” increases

ΔT = 15 fs

ω_1 = 1.5ω_0

Time delay increases

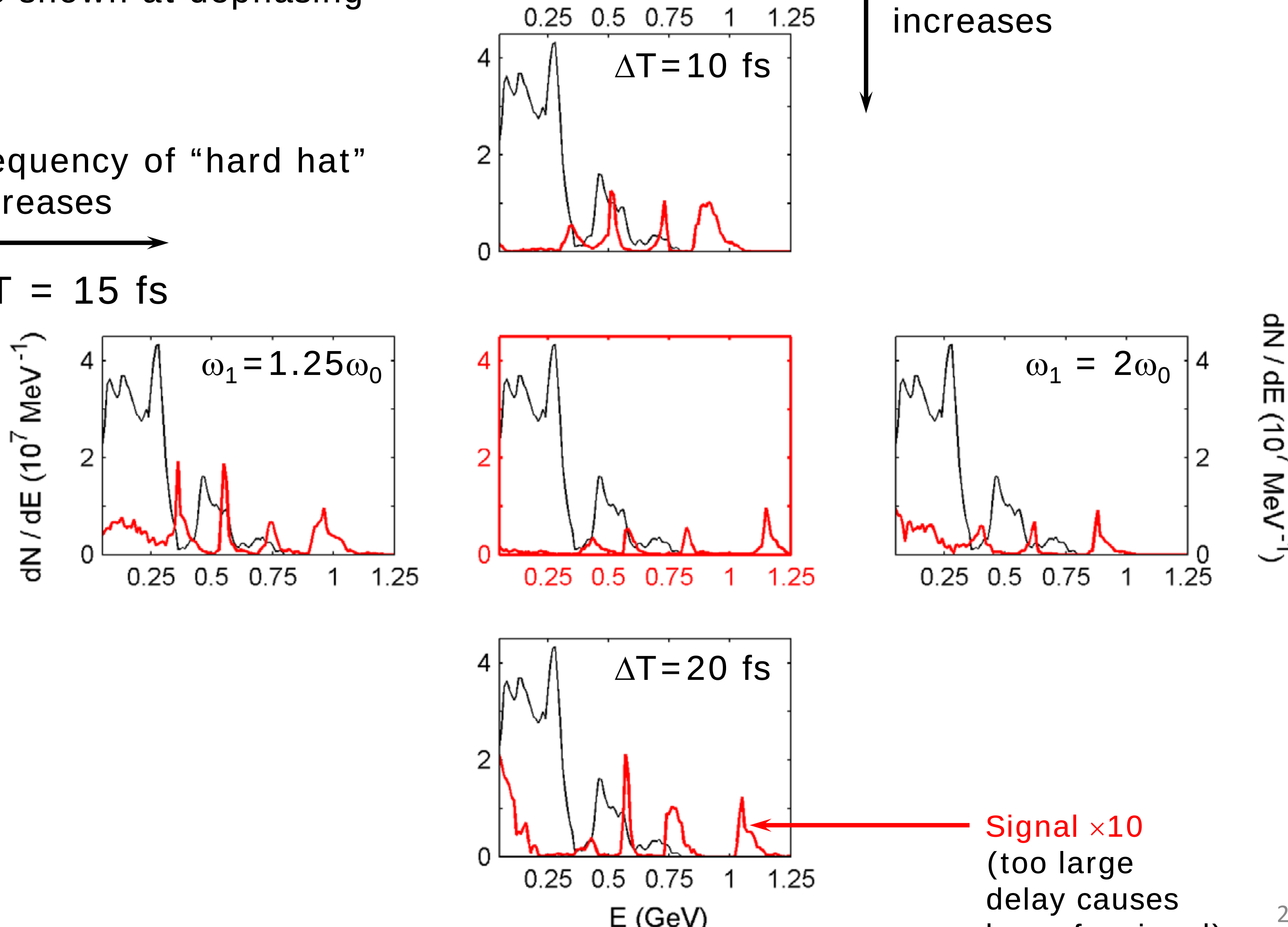

Signal ×10
(too large delay causes loss of a signal)

Stack in a channel — unequal energy partition

Electron energy spectra are shown at dephasing

Frequency of "hard hat" increases, energy drops

Time delay increases

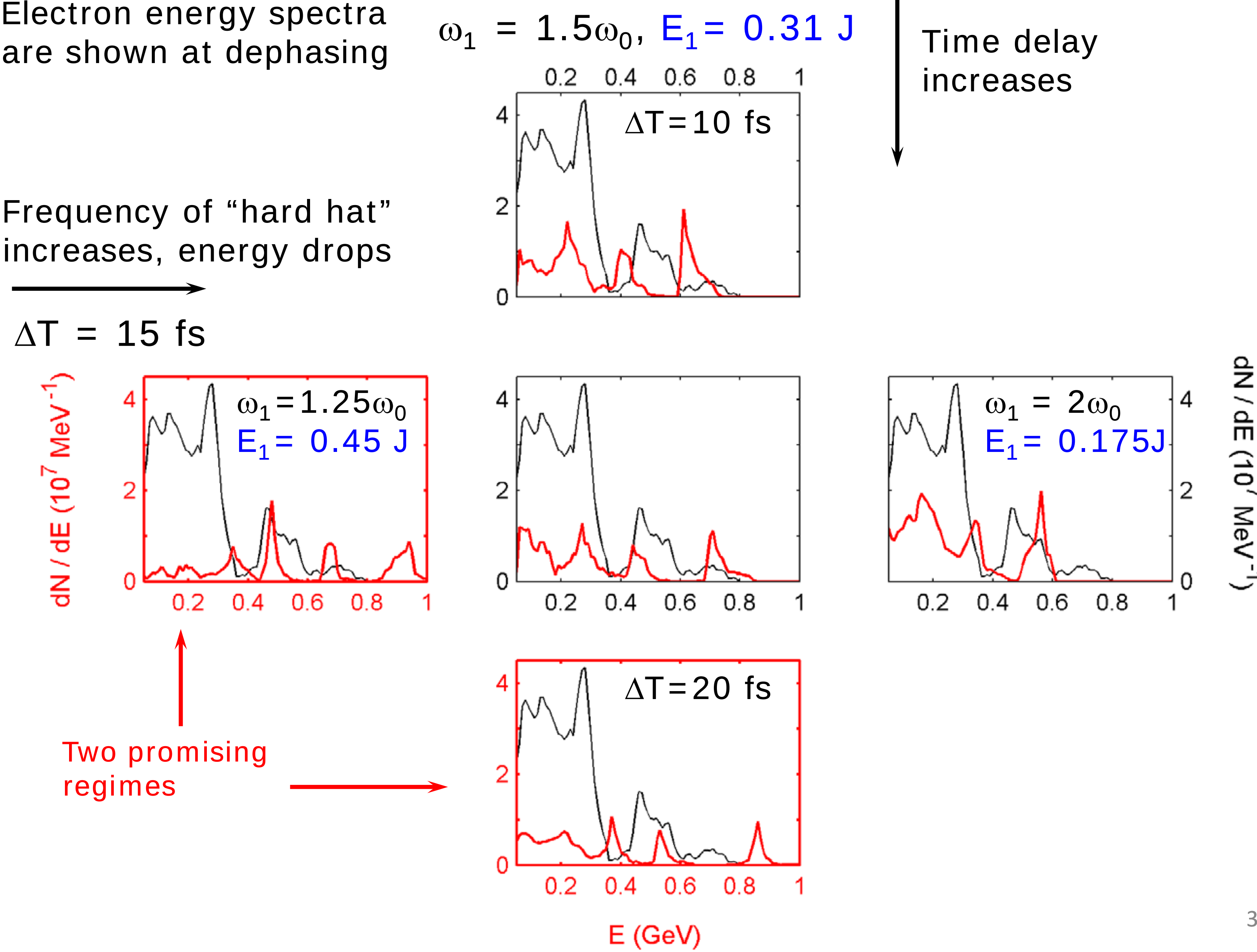

Stack with unequal energy partition: progress through dephasing in a channel

($\lambda_2 = 0.8\ \lambda_1$, $E_1 = 0.7$ J, $E_2 = 0.45$ J, delay +15 fs)

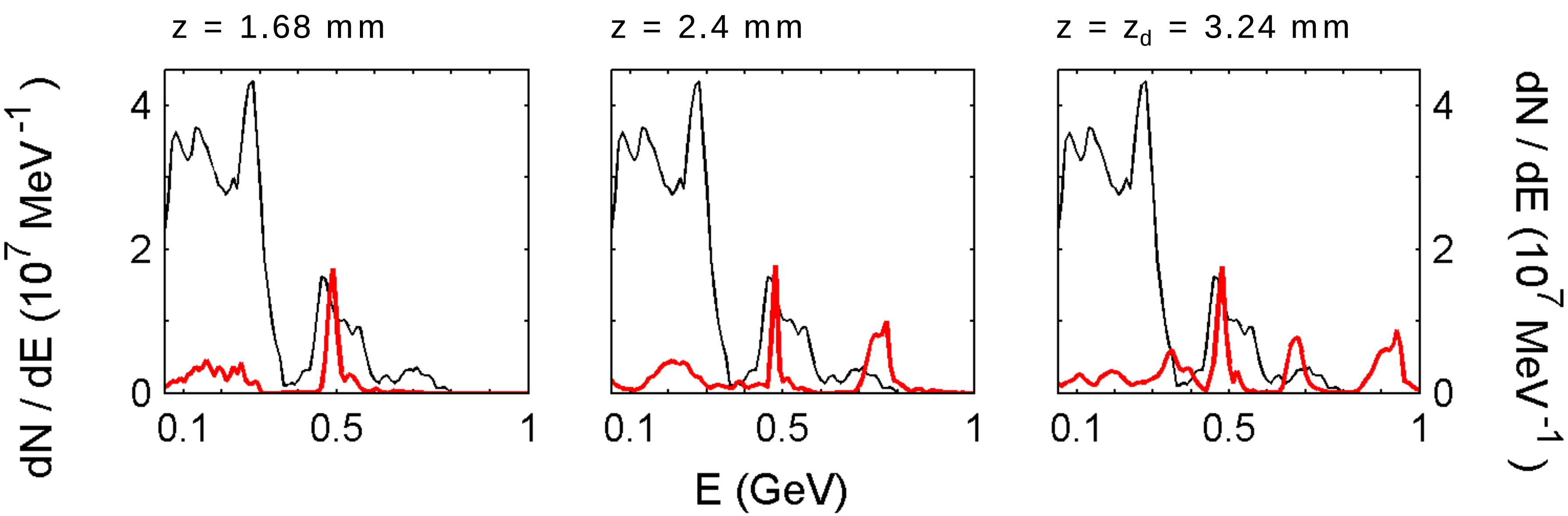

Changing the energy and frequency difference from the optimal values does not disrupt formation of the background-free, 4-component energy comb (the peak energy gain drops by ≈ 15%)

Summary

High-repetition-rate, GeV-scale LPAs generating femtosecond, multi-kA electron beams "by design" are critical elements of advanced radiation sources.

Building the drive pulse of independent sub-Joule, transform-limited pulses with large (up to ω_0) difference frequency permits an *unprecedented degree of electron beam phase space control.*

This photon engineering helps compensate for the nonlinear frequency shift imparted by the wake excitation, almost eliminating the dark current and boosting electron energy far beyond the predictions of the accepted scaling.

Propagation of the stacked driver in a channel leads to controllable generation of GeV-scale electron energy combs, while preserving sub-mm mrad emittance of individual bunches.

Monoenergetic (or comb-like) electron beams from stack-driven LPA are natural drivers for tunable, pulsed ITS sources of γ-rays.

LOOKING FORWARD TO EXPERIMENTAL REALIZATION!

OFFERS TO COLLABORATE ARE MOST WELCOME!

Additional info

GeV-scale designer beams from plasma channels (monochromatic or comb-like)

Laser	Plasma	e-beams from the 1st bucket (at dephasing)
30 fs, transform limited	Flat	1 QME bunch & bright tail 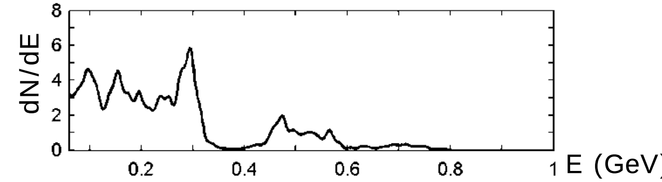
30 fs, negative chirp	Flat	1 QME bunch & weak tail 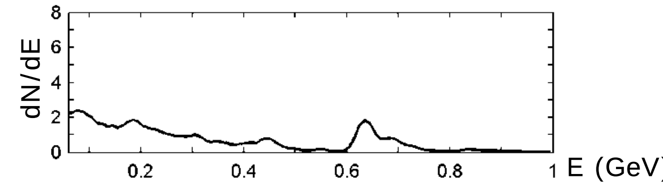
30 fs, negative chirp	Wide channel: matched to the incident pulse spot size	2 QME bunches & weak tail 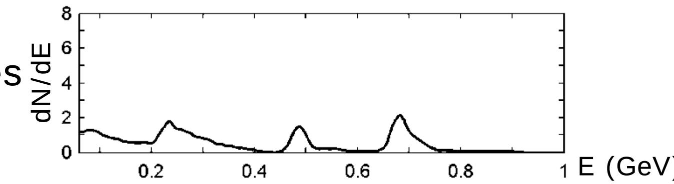
30 fs, negative chirp	Narrow channel: matched to the self-guided spot size	3 QME bunches & weak tail 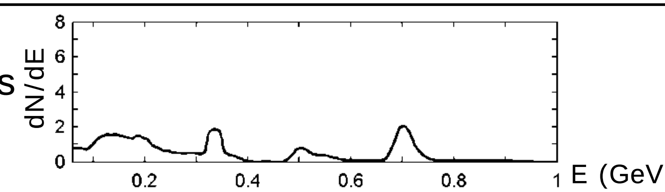
20 fs, negative chirp	Wide channel: matched to the incident pulse spot size	1 QME bunch & weak tail 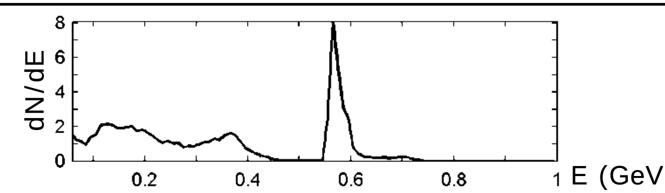

Simulation code: CALDER-Circ

Multi-color inverse Compton signal off tri-color electron beam

Dephasing in the channel (z_{acc} = 1.8 mm): 3 QME beams + weak tail

	#1	#2	#3	Tail
$\langle E \rangle$ ($\langle \Delta E \rangle$) (MeV)	770 (55)	580 (40)	405 (15)	-
σ_α (mrad)	2.15	3.4	3.2	> 7.5
$\varepsilon_{\perp,N}$ (mm mrad)	1.3	1.4	0.75	-
Charge (pC)	175	95	105	530
Average flux, $Q/\langle \Delta E \rangle$ (pC MeV^{-1})	3.2	2.375	7	1.7
Inverse Compton signal: E_{peak} (MeV) – estimated	12	7	3.5	-
Inverse Compton signal: ΔE_{FWHM} (MeV) – estimated	5	2.5	1	-
Inverse Compton signal: Average flux $\langle dN_{ph}/dE\, d\Omega \rangle$ (10^8 MeV^{-1} sr^{-1}) – estimated	0.7	0.5	0.5	0.2

Quasi-monochromatic inverse Compton signal off quasi-monoenergetic electrons from the channel

Dephasing in the channel (z_{acc} = 1.65 mm): 1 QME beam + weak tail

	#1	Tail
$\langle E \rangle$ ($\langle \Delta E \rangle$) (MeV)	585 (32)	-
σ_α (mrad)	2.6	> 8.5
$\varepsilon_{\perp, N}$ (mm mrad)	0.85	-
Charge (pC)	400	735
Average flux, $Q/\langle \Delta E \rangle$ (pC MeV^{-1})	12.5	1.5
Inverse Compton signal: E_{peak} (MeV) - estimated	7	-
Inverse Compton signal: ΔE_{FWHM} (MeV) - estimated	2	-
Inverse Compton signal: Average flux $\langle dN_{ph}/dE\, d\Omega \rangle$ (10^8 MeV^{-1} sr^{-1}) - estimated	2.5	0.35

Interaction pulse:
planar, linearly polarized wave, amplitude a_0 = 0.1, wavelength 0.8 μm, interaction length 250 fs. Detector: on axis, scattering angle = π.

Energy spread is $\Delta E_{FWHM}/E_{peak} \sim 3\times(2\langle \Delta\gamma/\gamma \rangle)$ $\Rightarrow$ energy spread of Compton γ-rays is defined by the electron beam divergence [P. Tomassini et al., Appl. Phys. B **80**, 419-436 (2005)].